doi:10.3772/j.issn.1006-6748.2014.03.011

Force modeling for needle insertion into soft tissue based on mechanical properties and geometric parameters①

Su Zhiliang (宿志亮)*, Jiang Shan②*, Wang Xingji*, Yan Yu**
(*Centre for Advanced Mechanisms and Robotics, School of Mechanical Engineering, Tianjin University, Tianjin 300072, P. R. China)
(**Department of Radiation Oncology, Thomas Jefferson University, Philadelphia 19107, U. S)

Abstract

The force model during needle insertion into soft tissue is important for accurate percutaneous intervention. In this paper, a force model for needle insertion into a tissue – equivalent material is presented and a series of experiments are conducted to acquire data from needle soft – tissue interaction process. In order to build a more accurate insertion force model, the interaction force between a surgical needle and soft tissue is divided into three parts: stiffness force, friction force, and cutting force. The stiffness force is modeled on the basis of contact mechanics model. The friction force model is presented using a modified Winkler's foundation model. The cutting force is viewed as a constant depending on a given tissue. The proposed models in the paper are established on the basis of the mechanical properties and geometric parameters of the needle and soft tissue. The experimental results illustrate that the force models are capable of predicting the needle-tissue interaction force. The force models of needle insertion can provide real-time haptic feedback for robot-assisted procedures, thereby improving the accuracy and safety of surgery.

Key words: force modeling, needle insertion, soft tissue, mechanical properties, geometric parameters

0 Introduction

Percutaneous intervention using surgical needles is a common minimally invasive procedure. The effectiveness of treatment is highly dependent on the accuracy of percutaneous insertion. To avoid human errors and improve the accuracy of insertion, robot-assisted needle steering, which is intended to guide the needle to the targeted locations deep within soft tissue, has become an active research area[1,2]. Therein, the tissue deformation and needle deflection that influence the precision of diagnosis and the effectiveness of surgery are affected by the needle-tissue interaction forces. Thus, the accurate force modeling is a foundation for the robot-assisted needle insertion.

The force model has been studied for realistic surgical simulation, preoperative planning, and robot-assisted medical procedures. Finite-element models, empirical models and fracture mechanics analytical models have been used to predict needle insertion force. DiMaio et al.[3] used a 2-D finite-element model to study the correlation between forces and deformations. Furthermore, the force distribution along the needle shaft was estimated via observed tissue deformations. Alterovitz et al.[4] obtained a dynamic contact model using the finite-element method with application to prostate brachytherapy. Okamura et al.[5] presented an empirical model based on the experimental measurement and characterized the effects of needle diameter and tip type on insertion force using a silicone rubber phantom. Asadian et al.[6] proposed a modified LuGre model for representing friction force using nonlinear dynamics. Based on sequential extended Kalman filtering, they derived an estimation algorithm for identifying parameters of the model. Azar et al.[7] developed a fracture mechanics model to predict the penetration force during quasi-static needle insertion into soft tissue. Of the force models mentioned above, only fracture mechanics analytical model specifically attempts to produce predictive model of needle insertion in view of the material properties. In contrast to the fracture mechanics, the

① Supported by the National Natural Science Foundation of China (No. 51175373), New Century Educational Talents Plan of Chinese Education Ministry (No. NCET-10-0625), Key Technology and Development Program of Tianjin Municipal Science and Technology Commission (No. 12ZCDZSY10600), and Tianjin Key Laboratory of High Speed Cutting & Precision Machining (TUTE) (2013120024001167).

② To whom correspondence should be addressed. E-mail: shanjmri@tju.edu.cn

Received on Mar. 6, 2013

model proposed here does not estimate the work of fracture nor determines the fracture toughness of the soft tissue. Instead, it relies on both the soft tissue and needle characteristics, such as the Young's modulus, Poisson ratio, and bevel angle.

The paper is organized as follows. Section 1 briefly introduces the experimental devices for studying the needle insertion in soft tissue. In Section 2, the force models are presented based on the contact mechanics and the modified Winkler's foundation. Moreover, the proposed force models are compared with experimental results to demonstrate the correctness of them. Finally, conclusions and future work are provided in Section 3.

1 Experimental data acquisition

Experiments have been designed to measure mechanical parameters of soft tissue and needles, and acquire experimental data for verifying the accuracy of the force models proposed in the following sections. Therefore, a 1-degree-of-freedom (DOF) experimental device fitted with a 6-DOF force/torque (F/T) sensor and surgical needle has been designed and fabricated for needle insertion into soft tissue. A 6-DOF F/T sensor (Nano-17) is mounted horizontally aligning its z-axis parallel to the setup's z-axis at the needle holder. A servo motor is used to define the speed and depth of insertion, and maintain the specified velocity during needle insertion. A tissue-equivalent material (PVA phantom) is used in this experiment which shares similar biomechanical characterizations and morphological structures with porcine kidney and is restrained by perspex cube container. Commercially available puncture needles are used which have 0.7mm in diameter (7G) and 80mm in length with beveled tip. The speed of needle insertion is acquired at the rate of 60 Hz while insertion force/torque data is recorded at the rate of 1kHz after being smoothed by an average filter. Experiments are carried out on artificial phantoms (PVA phantoms), since these artificial phantoms offer a controlled environment for repeatable experiments, consistent mechanical properties and being readily available at relatively low cost. The test-bed and PVA phantom for the experiments are shown in Fig. 1.

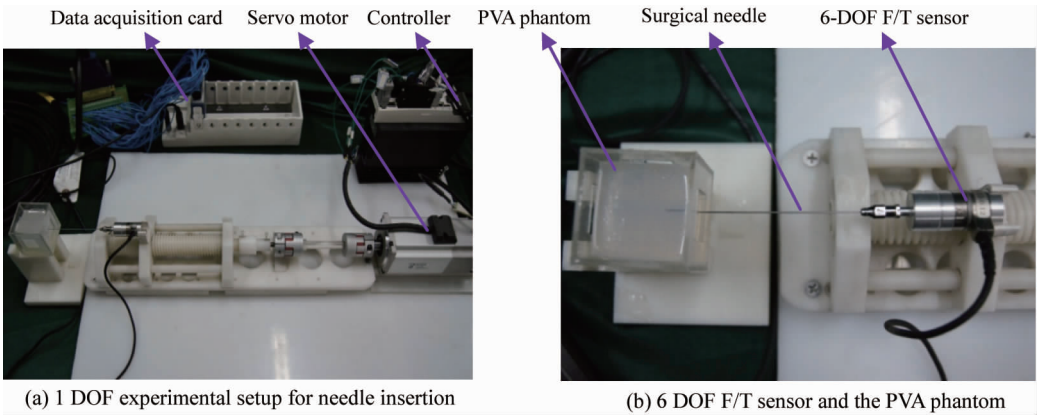

Fig. 1 (a) 1 DOF experimental setup for needle insertion. (b) 6 DOF F/T sensor and the PVA phantom

2 Modeling of needle-tissue interaction forces

Interaction forces are developed as a beveled needle inserted into the soft tissue. The force profile during needle insertion into the soft tissue is depicted in Fig. 2. Insertion force $F(z)$ is defined as the force acting on the needle in the direction of insertion. The forces of $F(x)$ and $F(y)$ which are perpendicular to the needle axis are caused mainly by asymmetric needle tip, and can be neglected because the values of them is relatively small. In order to accurately model the insertion force, Okamura et al. [5] have demonstrated that the insertion force is composed of stiffness, friction and cutting forces. Then, the insertion force $f_{\text{needle}}(z)$ is written as

$$f_{\text{needle}}(z) = f_{\text{stiffness}}(z) + f_{\text{friction}}(z) + f_{\text{cutting}}(z) \quad (1)$$

where z is the position of the needle tip relative to a fixed coordinate system before puncture happens. $f_{\text{stiffness}}(z)$, $f_{\text{friction}}(z)$ and $f_{\text{cutting}}(z)$ are the stiffness force, the friction force and the cutting force, respectively.

During needle insertion into the soft tissue, three basic phases of the needle-tissue interaction are distinguished as follows.

(1) Deformation phase (from A to B): Tissue deformation occurs when the needle comes into contact with the surface of soft tissue initially until the insertion force reaches the given energetic threshold. In this phase, the insertion force is equal to the stiffness force.

(2) Insertion phase (from B to C): The needle penetrates into the soft tissue. During the insertion phase, the measured insertion force is a summation of friction and cutting forces.

(3) Extraction phase (from C to D): The needle is extracted from the soft tissue. The insertion force is due to the friction force in this phase.

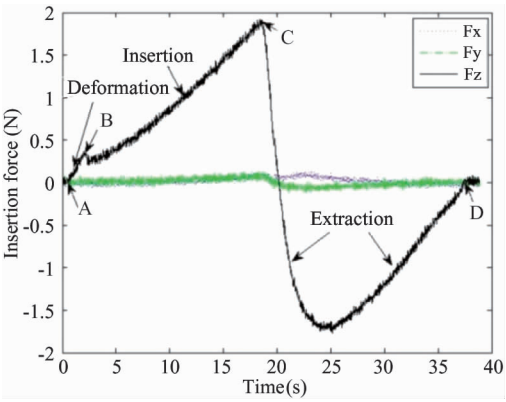

Fig. 2 Forces versus time curve for needle insertion into and removal from soft tissue at 3mm/s

2.1 Stiffness force

The stiffness force is due to the elastic properties of the organ and its capsule during the deformation phase, before the puncture in the surface. Many researchers have focused on the stiffness force and proposed various nonlinear models. Such as, Maurin, et al.[8] represented the stiffness force caused by the tissue deformation as an exponential function of the insertion depth. Simone, et al.[9] found that a second order polynomial well fitted to the measured force data. However, these models have been developed on the premise that the experiment data cannot represent combinations of tissue and needle characteristics, and so they required the determination of a new set of parameters to the different tissues or needles. We employ a contact model (see Fig. 3) here that accounts for both the needle and soft tissue mechanical characteristics to calculate the force-deformation response of a needle in contact with a soft tissue. The insertion force before puncture is reduced to a contact mechanic problem between soft tissue and needle.

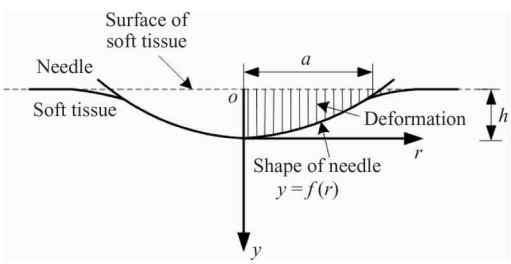

Fig. 3 The sketch of the contact model

The contact mechanic problem can be solved by means of a systematic use of Hankel transforms and the theory of dual integral equation. The elementary solution enables us to derive the expressions[10]

$$h = \int_0^1 \frac{f'(x)}{\sqrt{1-x^2}}\mathrm{d}x \tag{2}$$

$$f_{\text{stiffness}} = 2E_r a\int_0^1 \frac{x^2 f'(x)}{\sqrt{1-x^2}}\mathrm{d}x \tag{3}$$

in which function $f(x)$ is prescribed by the fact that, referring to the needle tip as the origin, the curve of needle is expressed as $y = f(r)$ where $r = ax(r \leqslant a)$ so that $f(0) = 0$; a is the radius of the circle of contact and h is a parameter whose physical significance is that it is the depth to which the tip of the needle penetrates into the soft tissue; E_r represents the reduced modulus that can be determined by

$$\frac{1}{E_r} = \frac{1-\upsilon_1^2}{E_1} + \frac{1-\upsilon_2^2}{E_2} \tag{4}$$

where E_1, E_2 and υ_1, υ_2 are the Young's modulus and the Poisson ratio of the needle and soft tissue, respectively.

The Young's modulus of the needle is estimated by measuring the force acting on the needle shaft and the deflection of the needle tip. On the basis of five experiments that apply the same force ($F = 0.1N$) at different positions of the needle, the Young's modulus of the needle is experimentally evaluated to 14.1GPa (standard deviation 1.6GPa). Ref. [11] presents a uniaxial tensile test for the sake of the Young's modulus of the soft tissue. Then the effective Young's modulus of the soft tissue is obtained which is equal to 116 KPa via the inverse solution through optimization toolbox in ANSYS.

Although Eq. (3) is the solution to the axisymmetric Boussinesq problem, the beveled-tip needle is analogous to the conical punch in that they are point contact with the soft tissue. For simplifying the formula of the stiffness force, we take $f(x) = \varepsilon x$ where $\varepsilon = a\cot\alpha$ for normal penetration by a bevel angle $\alpha = 15°$. Then the function $f(x)$ can be written as

$$f(x) = ax\cot\alpha \tag{5}$$

Substituting Eq. (5) and Eq. (2) into Eq. (3), the stiffness force is

$$f_{\text{stiffness}} = \frac{2}{\pi}E_r(\tan\alpha)h^2 \tag{6}$$

Based on the formula of the stiffness force, it is concluded that the mechanical properties of the needle and the soft tissue, as well as the needle bevel angle influence the stiffness force. The experimental data and stiffness force model are shown in Fig. 4.

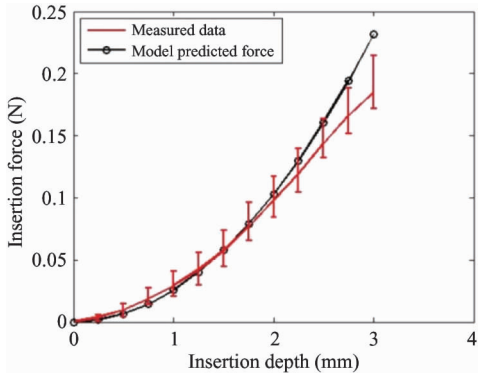

Fig. 4 The stiffness force for PVA phantom before puncture of the capsule

The figure clearly shows a non-linear increase in stiffness force before the puncture occurs due to inherent nonlinearity of tissue stiffness properties. The maximum soft tissue deformation and the stiffness force have been investigated. Based on the five experiments of needle insertions into the PVA phantom, the maximum stiffness force before puncture averages 0.2101N (standard deviation 0.0105N), occurring at an insertion depth of 3.2370mm (standard deviation 0.1347mm). The little standard deviations provide evidence for the homogeneous characteristic of PVA phantom in comparison with biological tissue.

2.2 Friction force

The friction force occurs along the shaft of the needle inside the tissue, and is due to Coulomb friction, tissue adhesion and damping. The measured force data of needle insertion consist of the friction and cutting forces. It is difficult to separate the friction force from the resultant force acting on the proximal end of the needle measured by the sensor directly. In order to acquire the friction force, a hypothesis has been proposed that the measured force is composed of the friction force only at the second insertion of two consecutive insertions at the same location. The needle force distribution indicates that axial forces between the needle and the tissue phantom are relatively uniform along the needle shaft[12], so it is reasonable to assume a linear lateral force responses for small displacement. Thus, the distributed force along the needle axis could be modeled as a modified Winkler's foundation[13] (see Fig. 5) with linear stiffness coefficient

$$F_n = kA\Delta \tag{7}$$

where F_n is the normal force along the needle shaft due to the tissue deformation, Δ is the settling amount, k is the foundation modulus and A refers to the contact area of the needle with soft tissue and is given as

$$A = \pi Dh \tag{8}$$

where h is the insertion depth and D is the outer diameter of needle.

Biot, et al.[14] has developed an empirical formula for k

$$k = \frac{0.65E_2}{1-\upsilon_2^2}\sqrt[12]{\frac{E_2 b^4}{E_1 I}} \tag{9}$$

where I and b are moment of inertia of the needle and foundation width, respectively.

The friction force acts on the side wall of the needle shaft in the axial direction is viewed as Coulomb friction. Then, the friction force can be expressed as

$$f_{\text{friction}} = \mu F_n \tag{10}$$

μ is the friction coefficient between needle and the soft tissue.

Substituting Eq. (7), Eq. (8) and Eq. (9) into Eq. (10). In this work, the friction is simplified using $\Delta = \frac{D}{2}$ and $b = \pi D$, the friction force model can be written as

$$f_{\text{friction}} = \frac{\pi\mu D^2}{2}\frac{0.65E_2}{1-\upsilon_2^2}\sqrt[12]{\frac{E_2(\pi D)^4}{E_1 I}}h \tag{11}$$

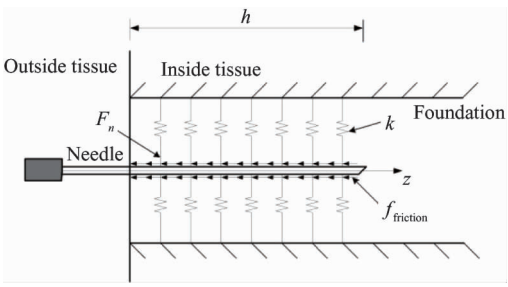

Fig. 5 Modified Winkler's foundation model

Fig. 6 presents the estimated friction force as well as the experimental data for PVA phantom. Eq. (11) indicates that the needle diameter and the material properties have an effect on the friction force. The experimental data demonstrate that the friction increases approximately and linearly with insertion depth in the

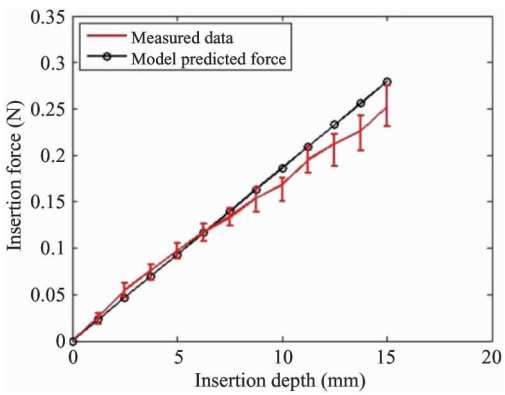

Fig. 6 The friction model predicted force and the measured force

PVA phantom. With the least square algorithm, the friction force density is found to be 0.0186N/mm. However, the prediction error becomes large when the needle penetrates into the soft tissue deeper more than 12mm, where the needle deflection and the force distribution along the needle shaft cannot remain uniform.

2.3 Cutting force

The measured force shows regular fluctuation when the needle is inserting into the soft tissue at 1mm/s (see Fig. 7(a)). The phenomenon is similar to stick-slip friction, most likely created by the needle status switch between pre-sliding and sliding regimes. The cutting force is necessary for the needle tip to slice through the tissue and it can be confirmed by subtracting the measured force of the second insertion from the total force.

As shown in Fig. 7(b), the cutting force ranges from 0.04N to 0.1N periodically, and it is found that the fluctuation can disappear when the insertion speed is equal to 3mm/s (as shown in Fig. 2) and the insertion forces of two consecutive insertions are parallel to each other. Therefore, the cutting force can be treated as a constant and unrelated to needle depth. For five needle insertions into the PVA phantom, the average cutting force f_{cutting} is equal to 0.0776N (standard deviation 0.0139N).

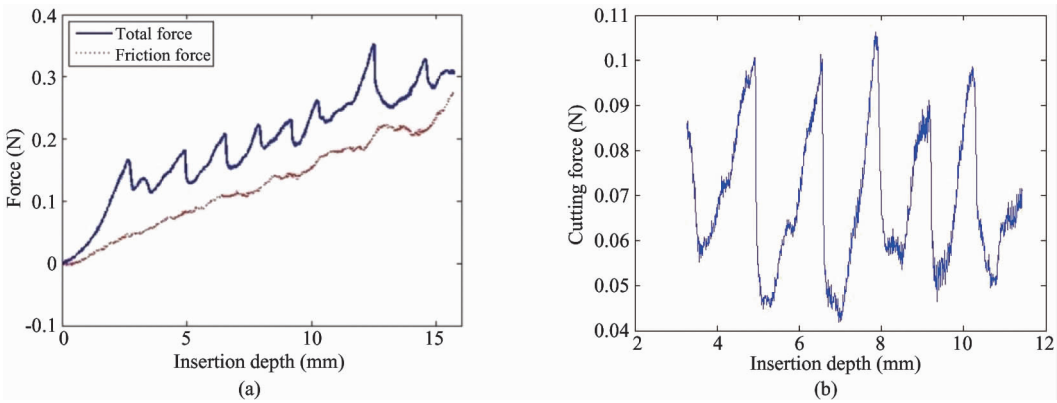

Fig. 7 (a) The force of two consecutive insertions at the same location; (b) The D-value of two consecutive insertion forces with insertion depth from 3.2mm to 11.2mm

2.4 Complete force model

Based on the parameter values obtained in the previous sections, a complete model of the needle insertion force profile is established.

$$f_{\text{needle}}(z) = \begin{cases} f_{\text{stiffness}} = \dfrac{2}{\pi} E_r \tan(\alpha) z^2 & z_A \leqslant z \leqslant z_B \\ f_{\text{friction}} + f_{\text{cutting}} = \dfrac{\pi\mu D^2}{2} \dfrac{0.65E_2}{1-\upsilon_2^2} \sqrt[12]{\dfrac{E_2(\pi D^4)}{E_1 I}} z + C & z_B \leqslant z \leqslant z_C \\ f_{\text{friction}} = -\dfrac{\pi\mu D^2}{2} \dfrac{0.65E_2}{1-\upsilon_2^2} \sqrt[12]{\dfrac{E_2(\pi D^4)}{E_1 I}} z & z_C \leqslant z \leqslant z_D \end{cases}$$

where z_A is the position of the undeformed tissue surface, z_B is the position of the maximally deformed tissue surface before puncture, z_C is the maximal insertion depth, z_D is the position where the needle separates from the soft tissue.

The simulated force and experimental force from real needle insertion have been compared, as shown in Fig. 8, and very good agreement between experimental data and computational results is observed. The overall shape of the model is coherent to the experimental results, although the fluctuations in the insertion phase make a perfect match impossible. In addition, we also make the assumption that the needle remains completely straight as it travels through the tissue, whereas there is small deflection that may affect the measured force in reality.

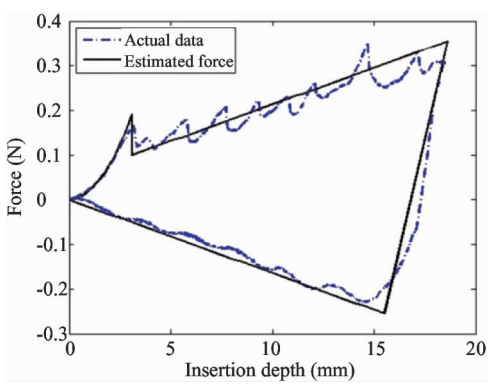

Fig. 8 The needle insertion model is compared to insertion on PVA phantom

3 Conclusions

In this work, needle-tissue interaction forces are identified for a bevel-tipped needle inserted into a PVA phantom. A novel stiffness force model has been proposed based on the contact mechanics model using the mechanical properties of needle and soft tissue. Additionally, the modified Winkler's foundation model is adopted to estimate the friction force when the needle penetrates into the soft tissue. The error between the force model and experimental results is caused by the nonlinearity of tissue stiffness and the deflection of the needle during insertion. Future work will explore the deflection function of puncture needle and consider the nonlinear properties of the soft tissue in Winkler's foundation model to improve the accuracy of the force model. However, compared with the needle insertion experiment, the estimated force was found to closely match the experimental data. Therefore, the mechanics-based model presented here is benefit to research needle steering into soft tissue, and it can be used to provide feedback for precise control of robot-assisted insertion.

References

[1] Abolhassani N, Patel R, Moallem M. Needle insertion into soft tissue: A survey. *Medical Engineering & Physics*, 2007, 29:413-431

[2] Sun Y S, Wu D M. Du Z J, et al. Modeling of needle insertion force in porcine livers for studying needle insertion strategies of robot-assisted percutaneous surgery. *Chinese High Technology Letters*, 2011, 21(9):948-953

[3] DiMaio S P , Salcudean S E. Interactive simulation of needle insertion models. *IEEE Transactions on Robotics*, 2005, 52(7):1167-1179

[4] Alterovitz R, Goldberg K, Pouliot J, et al. Needle insertion and radioactive seed implantation in human tissues: Simulation and sensitivity analysis. In: Proceedings of the 2003 IEEE International Conference on Robotics & Automation, Taipei, China, 2003. 1793-1799

[5] Okamura A M, Simone C, O'Leary M D. Force modeling for needle insertion into soft tissue. *IEEE Transactions on Biomedical Engineering*, 2004, 51(10): 1707-1716

[6] Asadian A, Patel R V, Kermani M R. A novel force modeling scheme for needle interaction using multiple Kalman filters. *IEEE Transactions on Instrumentation and Measurment*, 2012, 61(2):429-438

[7] Azar T, Hayward V. Estimation of fracture toughness of soft tissue from needle insertion. In: Proceedings of the 4th International Symposium Biomedical Simulation. (Lecture Notes in Computer Science, F Bello and E Edwards). London, UK, 2008. 166-175

[8] Maurin B, Barbe L, Bayle B, et al. In vivo study of forces during needle insertions. In: Proceeding of the Scientific Workshop on Medical Robotics, Navigation and Visualization, Remagen, Germany, 2004. 415-422

[9] Simone C, Okamura A M. Modeling of needle insertion forces for robot-assisted percutaneous therapy. In: Proceeding of the IEEE International Conference on Robotcis and Automation, Washington DC, USA, 2002. 2085-2091

[10] Sneddon L N. The relation between load and penetration in the axisymmetric Boussinesq problem for a punch of arbitrary profile. *International Journal of Engineering Science*, 1965, 3(1):47-57

[11] Jiang S, Liu S, Feng W H. PVA hydrogel propertied for biomedical application. *Journal of the Mechanical Behavior of Biomedical Materials*, 2011, 4(7):1228-1233

[12] DiMaio S P, Salcudean S E. Needle insertion modeling and simulation. *IEEE Transactions on Robotics and Automation*, 2003, 19(5):864-875

[13] Yankelevsky D Z, Eisenberger M. Analysis of beams on nonlinear winkler foundation. *Computers & Structures*, 1989, 31(2): 287-292

[14] Fischer F D, Gamsjager E. Beams on foundation, Winkler bedding or half-space-a comparison. *Technische Mechanike*, 2008, 2: 152-155

Su Zhiliang, born in 1988. He received the B. S degree in Mechanical Engineering from Qingdao University in 2011. He received the M. S degree in School of Mechanical Engineering of Tianjin University. His current research interests include medical robotic and image processing.